Analysis of passive magnetic bearings for kinetic energy storage systems

Elkin Rodriguez[a], Juan de Santiago[b], J. José Pérez-Loya[b], Felipe S. Costa[a], Guilherme G. Sotelo[c], Janaína G. Oliveira[d], Richard M. Stephan[a]

[a] Universidade Federal do Rio de Janeiro, Technology Center I-148, CEP 21941-909, Rio de Janeiro – RJ, Brazil,
elkinrodvel@msn.com
[b] Uppsala University, Ångström laboratory, 751 21, Uppsala, Sweden
[c] Fluminense Federal University, Passo da pátria Street 156 – room 431-E, CEP 24210-240 Niterói – RJ, Brazil
[d] Universidade Federal de Juiz de Fora, Cidade Universitária – Plataforma 5 Martelos, CEP 36036-900, Juiz de fora – MG, Brazil

***Abstract*— This paper describes a passive magnetic bearing system intended to be used in a flywheel. The upper bearing consists of two rings of permanent magnets operating as a radial bearing. The lower bearing consists of high temperature superconductors in the stator and a permanent magnet cylindrical disk in the rotor, which contributes to the radial and axial stability of the system. Those bearings have been tested in an experimental rig specially designed for it. Measurements of the radial and axial forces, both static and dynamic, for different gaps are presented in this paper**

I. INTRODUCTION

Flywheel Energy Storage Systems (FESS) are globally gaining attention. They raised in popularity when a FESS was introduced in Formula 1 in 2009 [1][2]. Other applications include electric grid voltage and frequency regulation [3], energy storage and load leveling for integration of renewable energy sources, as solar and wind power [4].

Energy storage systems are classified according to their energy capacity, power rate, life time, availability factor, etc. Flywheels are an environmentally friendly storage solution since no hazardous materials are used in their construction, resulting in a small environmental impact. But, on the other hand, high performance flywheels can only be achieved with magnetic bearings.

Flywheels store energy in form of rotational energy as presented in Eq. 1.

$$E = \frac{1}{2} I \omega^2 \tag{1}$$

High rotational speed increases energy density but also increases bearing losses. Magnetic bearings are therefore an interesting alternative to traditional rolling bearings. Magnetic Bearings can be classified into two major types: Active Magnetic Bearing (AMB) and Passive Magnetic Bearing (PMB). AMB requires accurate control of the current through the windings of electromagnets. PMB uses the repulsion forces without active control systems. The main advantages of PMB are the low energy consumption.

The authors are investigating the bearing set up presented in Fig. 1. The upper bearing is a permanent magnet bearing, and it consists of two rings of axially oriented permanent magnets. The lower bearing is a Superconducting Magnetic Bearing (SMB), and it is composed by melt textured $Y_1Ba_2Cu_3O_{7-\delta}$ superconductor (YBCO) in the stator and a rotor made with permanent magnets and steel arranged in a flux collector configuration.

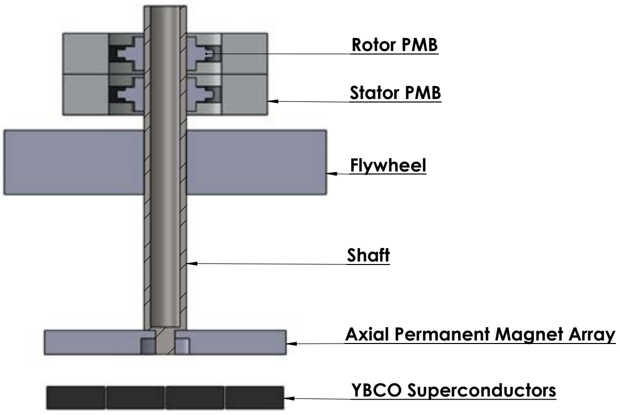

Figure 1. Schematic representation of the pasive magnetic bearing system.

The upper radial magnetic bearing properties were presented in [5]. The results of the static and dynamic tests to characterize the lower passive magnetic bearing are reported in the present paper.

The SMBs present different properties than rolling bearings and AMBs. They have lower force density and require broader air gaps. SMBs present limitations concerning the weight of the flywheel and the air gap required to motor/generator.

II. MAGNETIC BEARINGS STRUCTURE

The magnetic bearing system is presented schematically in Fig. 1. It consists of two PMB: one radial permanent magnet bearing on the top and one SMB in the bottom. This section presents details of the bearings' designs.

A. *Axial superconducting magnetic bearing*

The SMB is made up of 8 YBCO bulks enclosed in a static cryostat. The dimensions of each bulk are 67x32x14 mm^3, approximately. Fig. 2 shows two individual YBCO bulks and the complete array mounted inside the cryostat.

A disc made with Nd-Fe-B permanent magnets arranged and a soft ferromagnetic material arranged in an axial flux collector topology is mounted on the rotor [6][7]. The layout and dimensions of this setup are shown in Fig. 3.

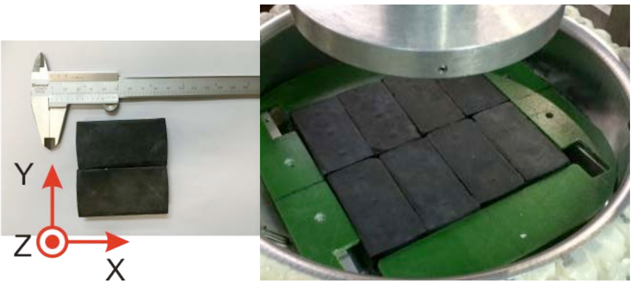

Figure 2. Superconductor blocks.

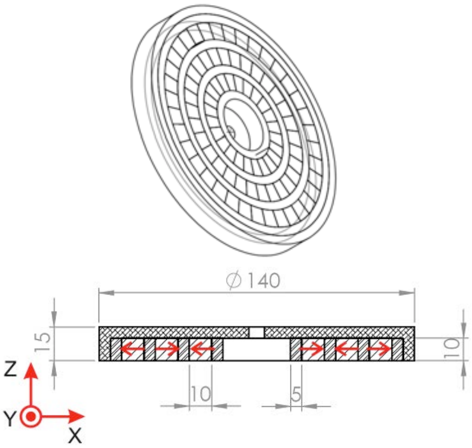

Figure 3. Axial flux concentrator permanent magnet array for the rotor of the supermconductive magnetic bearing.

B. *Radial permanent magnetic bearing (RPMB)*

This bearing is constructed by two concentric permanent magnet rings. This structure was previously investigated in [5], [8] and [9]. The main parameters of the upper radial magnetic bearing are summarized in Table I and Fig. 4.

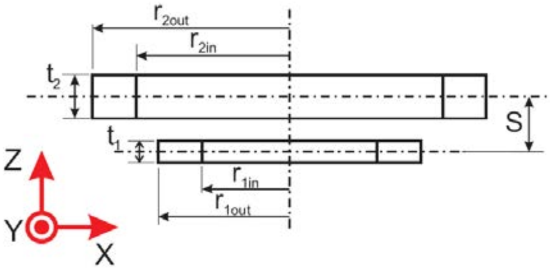

Figure 4. Parameterization of ring magnets used for the construction of the proposed Passive Magnetic Bearings.

TABLE I. RADIAL PERMANENT MAGNETIC BEARING

Parameters	Description	Length (mm)
r_{1in}	Inner radius of inner ring	20
r_{1out}	Outer radius of inner ring	30
t_1	Thickness of inner ring	5
r_{2in}	Inner radius of outer ring	35
r_{2out}	Outer radius of outer ring	45
t_2	Thickness of outer ring	10
S	Axial distance from geometric center of each magnet	--

III. PMB TEST RESULTS

The measurements were performed in a test bench that can be moved in the X and Z axes while a load cell is fixed over it, as shown in Fig. 5. This structure has two linear actuators, a six-axis (it measures X, Y and Z forces and X, Y and Z torques) ATI load cell and the National Instruments PCI-6040E board.

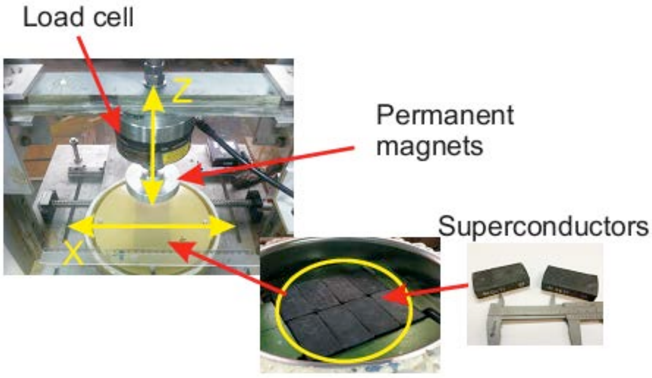

Figure 5. Measurement system.

A. *Radial permanent magnetic bearing (RPMB)*

The rotor has no physical contact with the stator. Therefore, the rotor can move in both radial and axial directions. The stator of the radial bearing was fixed in the test bench; the rotor was displaced from the stator center and the resulting force registered. This test was performed both for the axial and radial direction. Fig. 6 shows that the force measured suffers small variations also due to displacements in orthogonal directions. The radial direction has a positive stiffness, while the axial direction has a negative stiffness; the RPMB is therefore unstable in the axial direction and requires either active control or a stabilizing lower bearing.

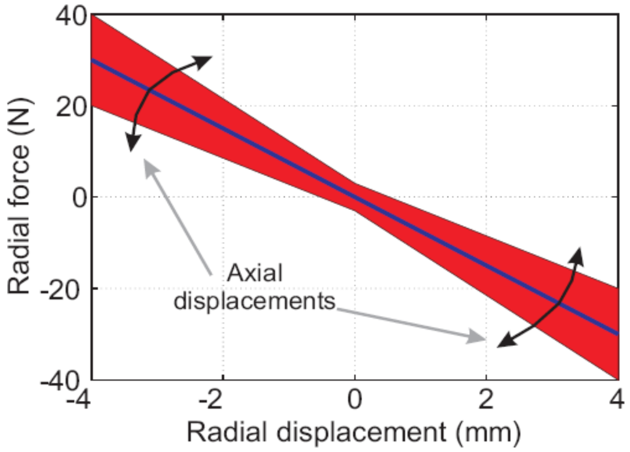

(a)

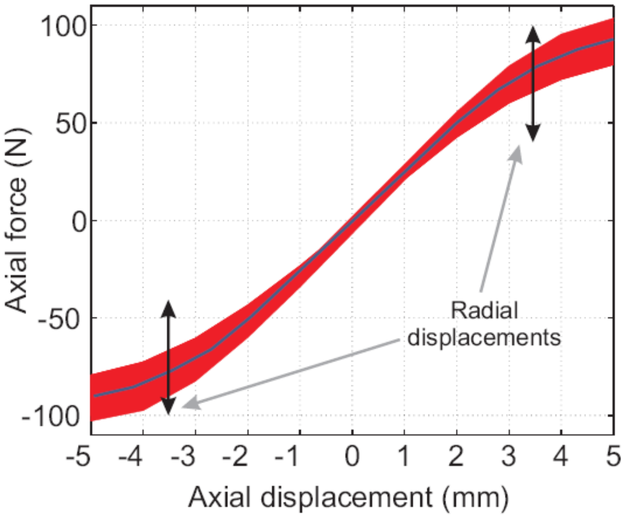

(b)

Figure 6. Behavior of the axial and radial forces for small axial and radial displacements.

B. *Axial superconducting magnetic bearing*

Superconductors present their diamagnetic and zero resistance effects only when they are cooled below a certain critical temperature. Liquid nitrogen was used in order to cool down the YBCO bulks in these experiments. When the superconductor is cooled in the presence of a magnetic field, the process is referred as field-cooling (FC). Zero field cooling (ZFC) means that the permanent magnet rotor is removed from the test set up when the superconductors were cooled down. Both FC and ZFC tests have been performed.

1) *ZFC static*

Rotor and stator were taken apart 130 mm before the superconductive material was cooled down below its critical temperature. After the cool down, the magnetic rotor was moved in a quasi-static movement, in steps of 1 mm. After each movement, the system remains static during one second in order to the flux can relax inside the superconductor. Fig. 7 shows the measured axial forces when the air gap was reduced and increased, forming a hysteresis loop.

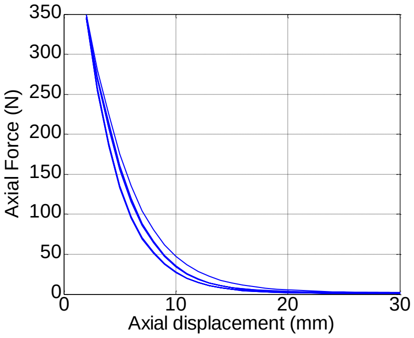

Figure 7. Axial force for different air gaps. ZFC test.

2) *FC static*

The superconductive material was cooled down below its critical temperature in the presence of a magnetic field. The rotor was lifted a certain distance while the stator was cooled down. The static tests have been performed in two steps after FC: the magnetic flux pumping and the displacement from the operation point. The process is explained in Fig. 8. The experiment was repeated for 4 different distances of FC so that we had different behaviors of magnetic field strength. The closer the rotor is to the superconductive element, the higher the magnetic field strength.

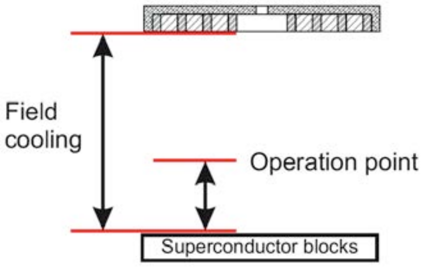

Figure 8. Schematic representation of the static tests of the superconducting magnetic bearing.

Figure 9 shows the magnetic flux pumping accomplished for each FC point, 12, 17, 22 and 27 mm between the rotor and the YBCO bulks.

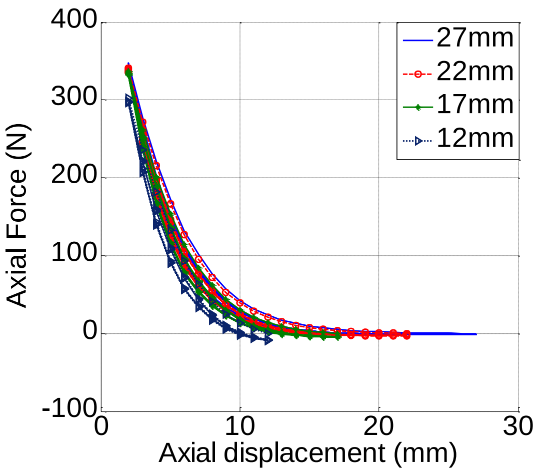

Figure 9. Axial force for different FC points.

The second test led the rotor to the operation point. This is located at 7 mm from the upper face of the superconductor blocks. Two different displacements were performed: the radial and axial displacements.

Smaller displacements in axial direction were accomplished to assess the behavior of the axial force. Figure 10 shows the axial force to each FC.

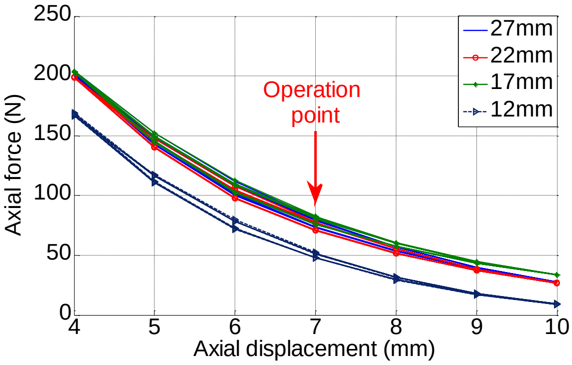

Figure 10. Axial force to small axial displacements in the operation point.

The radial stability has also been studied. The rotor was misaligned from the center of stator in X direction. Radial displacements with an amplitude of 5 mm were performed. Figure 11 shows the behavior of the radial force for these displacements for each FC height.

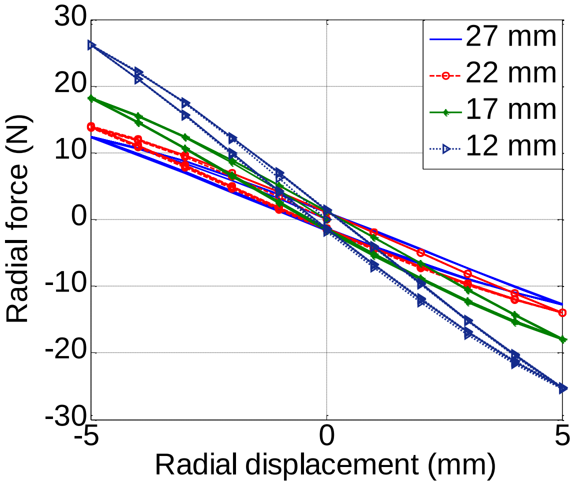

Figure 11. Radial force produced by each FC in the operation point.

3) Dynamic test

Dynamic tests were performed to assess the behavior of the SMB without any upper bearing. The test bench used to measure the force is shown in Fig. 12.

The FC height was 12 mm. After FC, the rotor was accelerated to 2650 rpm with the external help of a drill machine. At this speed, the rotor was released free. Figure 13 shows the speed decrease vs. time.

The radial and axial forces are shown in Figs. 14 and 15.

The passage through resonance frequencies can be clearly observed.

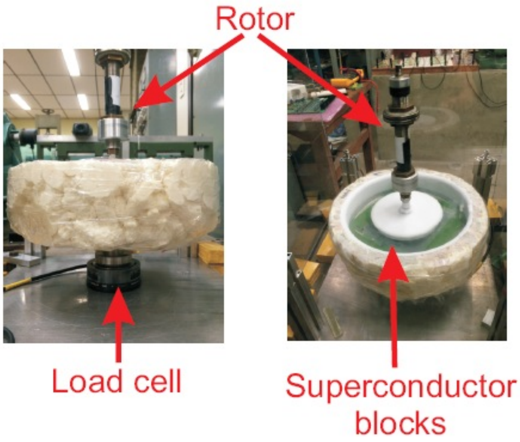

Figure 12. Superconducting magnetic bearing system to measure forces.

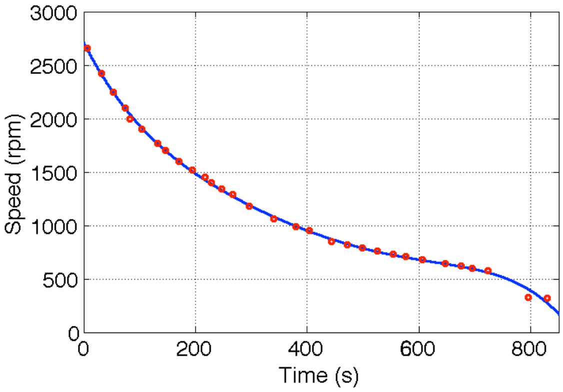

Figure 13. Speed decrease vs. time

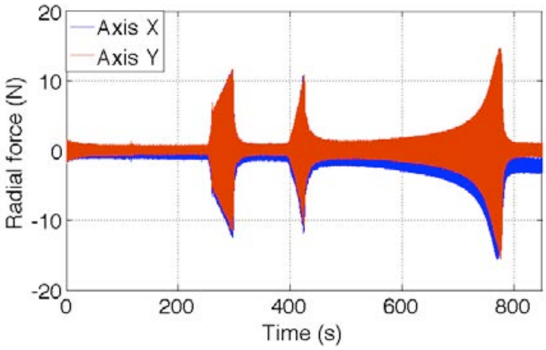

Figure 14. Radial forces vs. time.

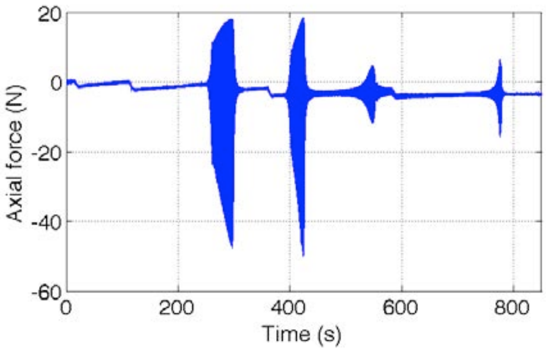

Figure 15. Axial force vs. time.

IV. DISCUSSION

Another configuration with 2 superconducting bulks has also been tested. Static results are presented in Figs. 16 and 17 to show the behavior of axial and radial forces interaction due to radial and axial displacements. These results were obtained with FC 20 mm. Axial force is measured for different air gaps and different radial displacements, and the influence of the radial displacement is not significant and only observed for big radial displacements.

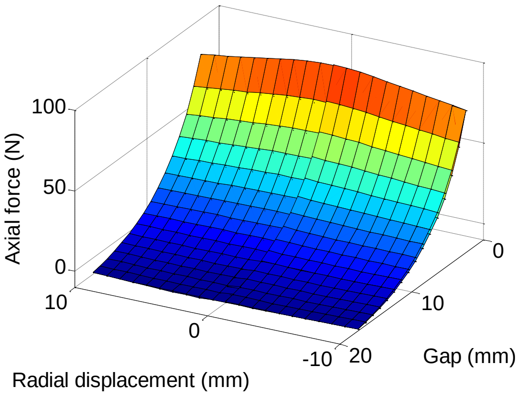

Figure 16. Axial force meassured due to axial displacement for different radial displacements. The test was performed with only 2 superconductive bulks in the SMB stator.

The radial force was also measured for different air gaps and the results are presented in Fig. 13. The SMB presents a non-linear region for small air gaps, but the radial force is independent from the air gap when a value of 7 mm or higher was chosen. This non-linear region is probably due to the small size of the superconductive array.

V. CONCLUSION

A passive magnetic bearing set up with a radial magnetic bearing on the top and a superconducting magnetic bearing on the bottom was presented. The bearings have been tested independently and the results were presented.

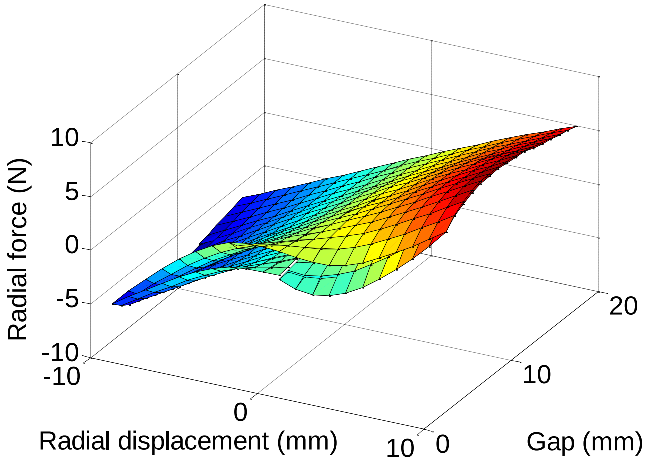

Figure 17. Radial force meassured for different axial and radial displacements. The test was performed with only 2 superconductive blocks in the SMB stator.

Radial permanent magnet bearings are intrinsically unstable, as the force increases proportionally to the displacement in the axial direction. They require some element to give stability to the set up, such as active control, a rolling bearing in the other side of the shaft or a superconducting magnetic bearing as applied in our set up.

The superconducting magnetic bearing constructed consists of a stator with an array of 8 pieces of high temperature superconductors (YBCO) and an axially-oriented permanent magnet flux concentrator array rotor. The test includes axial and radial force measurements with zero field cooling and field cooling in static and dynamic conditions.

The results have show that the SMB radial force with 12 mm FC (fig. 11) is similar to the results that obtained for RPMB (Fig. 6). The radial force increases for lower FC heights (Fig.11), however, the axial force decreases (Fig. 9 and 10).

For the complete implementation with passive magnetic bearings, the SMB with 12 mm FC is a good option, since it presents a similar radial force behavior to that of the RPMB. Moreover, the axial force is reduced but its rate of increase is bigger that with RPMB. Tests are under course and will be reported in the near future.

ACKNOWLEDGEMENTS

The authors would like to thank the financial support received from FAPERJ, Swedish Research Council, The Swedish Centre for Smart Grids and Energy Storage (SweGRIDS), STandUP for Energy and CONACYT.

REFERENCES

[1] J. Cibulka, “Kinetic energy recovery system by means of flywheel energy storage”, Advanced Engineering, vol 3, n.1, p. 27-38, 2009.

[2] A. A. Boretti, “Improvements of vehicle fuel economy using mechanical regenerative braking”, International Journal of Vehicle Design”, vol. 55, n. 1, p. 35-48, 2011.

[3] R. de Andrade, *et al.* “Flywheel energy storage system description and tests”, IEEE Transactions on applied superconductivity , vol. 17, n. 2, p. 2154-2157, 2007.

[4] J. M. Carrasco, *et al.*, “Power-electronic systems for the grid integration of renewable energy sources: A survey”. IEEE Transactions on Industrial Electronics, vol. 53, n.4, p. 1002-1016, 2006.

[5] E. Rodriguez and R. Stephan, “Study of Passive Magnetic Bearings for Vertical-Axis Wind Turbines”, 13 th International symposium on magnetic bearings, Arlington – USA, no. 32, august 7-9, 2012.

[6] G. G. Sotelo, A. C. Ferreira ans R. de Andrade, “Halbach Array Superconducting Magnetic Bearing for a Flywheel Energy Storage System“, IEEE Transactions on applied superconductivity, vol. 15, no. 2, June 2005.

[7] G. G. Sotelo, R. de Andrade and A. C. Ferreira, “Magnetic Bearing sets for a Flywheel System”, IEEE Transactions on applied superconductivity, vol. 17, no. 2, June 2007.

[8] E. Rodriguez and R. Stephan, “Radial and axial forces of a passive magnetic bearing”, 1st Brazilian workshop on magnetic bearings, Rio de janeiro – Brazil, no. 22, october 25-26, 2013.

[9] J. J. Pérez-Loya, et. al, “Magnetic Modeling and measurement of forces between permanent magnet rings used as passive magnetic bearings”, 1st Brazilian workshop on magnetic bearings, Rio de janeiro – Brazil, no. 25, october 25-26, 2013.